AUCTORES
Globalize your Research

Journal of Surgical Case Reports and Images

Nan Lu *

Open Access

Research Article

Theoretical investigation on BF_3·OEt_2-catalyzed tandem benzannula-tion/Friedel–Crafts reaction of 2-alkynylaniline and 2-alkynylbenzaldehyde delivering highly π-extended dihydroben-zo[a]indenocarbazole

Nan Lu *, Chengxia Miao

College of Chemistry and Material Science, Shandong Agricultural University, Taian 271018, P. R. China

***Corresponding Author:** Nan Lu, College of Chemistry and Material Science, Shandong Agricultural University, Taian 271018, P. R. China

Received Date: September 24, 2024; **Accepted Date:** October 10, 2024; **Published Date:** October 16, 2024

Citation: Nan Lu, Chengxia Miao, (2024), Theoretical investigation on BF_3·OEt_2-catalyzed tandem benzannula-tion/Friedel–Crafts reaction of 2-alkynylaniline and 2-alkynylbenzaldehyde delivering highly π-extended dihydroben-zo[a]indenocarbazole, *J, Surgical Case Reports and Images*, 7(9); **DOI:10.31579/2690-1897/217**

Abstract

Our DFT calculations provide the first theoretical investigation on BF3·OEt_2-facilitated benzannulation/Friedel–Crafts reaction of 2-(phenylethynyl) aniline with 2-(phenylethynyl)benzaldehyde. Imine is formed mediated by BF_3·OEt_2 via initial two steps. The subsequent nucleophilic attack from alkyne group of 2-(phenylethynyl) aniline forms the first alkenyl carbocation and five-membered ring continuously activated by BF3·OEt_2. With additional proton, the second alkenyl carbocation is given by attack from alkyne group of 2-(phenylethynyl)benzaldehyde together with novel six-membered ring. Then intramolecular Friedel–Crafts reaction and aromatization give rise to the second five-membered ring. The product dihydrobenzo[a]indeno[2,1-c] carbazole is finally obtained via 1,5-H shift, which is determined to be rate-limiting owing to the tension resulting from great structure bending required by long-distance shifting. The positive solvation effect is suggested by decreased absolute and activation energies in solution compared with in gas. These results are supported by Multiwfn analysis on FMO composition of specific TSs, and MBO value of vital bonding, breaking.

Keywords: Lewis Acid; benzannulation; friedel–crafts; π-extended; carbazole

1 Introduction

As privileged tricyclic nitrogen-containing hetero-cyclic motifs, carbazoles involve carbon skeleton of fluorene [1]. Polymers based upon 2,7-disubstituted carbazole function as electron-donating materials in organic photovoltaic devices [2]. They are also active compounds pharmaceutically and exist widely in alkaloid-based natural products [3-5], such as application in synthesis of carbazomycin A, calothrixin B, and staurosporinone. Its electron-rich and conjugated nature makes it prime as optoelectronic materials and organic fluorescent sensors with aggregation induced emission for detection of cyanide anion and Hg2+-protein binding [6,7]. Chen reported an indole-to-carbazole strategy under metal-free conditions for synthesis of carbazole derivatives demonstrating various biological activities including antimicrobial, anticancer and enzyme inhibition properties [8]. The stability and reactivity of carbazole are distinctive with a structure of two benzene rings fused to pyrrole ring [9]. Benzo[a]carbazoles are especially important among large varieties of carbazoles [10].

Benzo[a]carbazole is well known as core structure of bioactive products and key building blocks of organic materials. Paramasivam reported the influence of π-spacers in tuning the photovoltaic performance of benzocarbazole-based sensitizers for dye-sensitized solar cells [11]. Ivaniuk analyzed highly luminous sky-blue organic light-emitting diodes based on bis [(1,2)(5,6)] indoloanthracene emissive layer [12]. Furthermore, its derivatives are also widely used in pharmaceutical. For example, Ghanbari achieved direct synthesis of benzo [a] carbazoles by Palladium-catalyzed domino reaction and revealed photophysical properties to be agonists of human thrombopoietin receptor [13]. Kuo exploited dual character of benzoquinone as oxidizing agent and dienophile with powerful antitumor activities [14]. There is also Jeon's cyanide-catalyzed imino-stetter reaction/Friedel–Crafts reaction sequence and Yuan's Rhodium-catalyzed C–H activation/carbenoid insertion/Aldol-type cyclization [15,16]. Hence much interest has been focused on exploring efficient synthetic methods from materials readily available [17,18]. Such as the progress of Peng's Gold (I)-catalyzed

tunable domino cyclization of difunctional 1, 2-diphenylethynes and Rh(III)-catalyzed [5+1] annulation of 2-aryl-3-acyl-1H-indoles with a-diazo carbonyl compounds [19,20].

In spite of recent advancements for diverse heterocycles, the metal-free tandem protocols are relatively few as far as we know. Besides intramolecular aza-prins type reaction and stereoselective cascade alkynyl prins cyclization of Biswas group [21,22], there are unwavering commitments contributed by Chutia including temperature tunable synthesis of tetrahydro-4H-pyrrolo[3,2-c] quinolin-4-ones and tandem oxidation/iodolactonization of 2-O/N-tethered alkenyl benzaldehyde in this aspect [23,24]. Considering the merits of 2-Alkynylaniline and 2-Alkynylbenzaldehyde, a breakthrough was Chutia's Lewis acid (LA)-catalyzed tandem benzannulation and Friedel−Crafts reaction [25]. Although highly π-extended dihydrobenzo[a]indenocarbazole were yielded, many problems still puzzled and there was no report about detailed mechanistic study explaining the promotion of $BF_3{\cdot}OEt_2$. How the vital imine intermediate is formed initially mediated by $BF_3{\cdot}OEt_2$ and undergoes further activation? How alkenyl carbocation is obtained via two times of nucleophilic attack? What's specific process of the last significant 1,5-H shift from intermediate of intramolecular Friedel−Crafts reaction? To solve these questions in experiment, an in-depth theoretical study was necessary for this strategy also focusing on the comparison of uncatalyzed paths and photophysical properties of products.

2 Computational details

Optimized structures were obtained at M06-2X/6-31G(d) level of theory with GAUSSIAN09 [26]. In tests of popular DFT methods [27], M06-2X functional attained smaller standard deviation of difference between calculated value and experimental value in geometries than B3LYP including Becke's three-parameter hybrid functional combined with Lee−Yang−Parr correction for correlation [28,29]. The best compromise between accuracy and time consumption was provided with 6-31G(d) basis set on energy calculations. Also, M06-2X functional was found to give relatively accurate results for catalysed enantioselective (4 + 3), concerted [4 + 2], stepwise (2 + 2) cycloaddition and catalysed Diels−Alder reactions [30,31]. Together with the best performance on noncovalent interaction, M06-2X functional is believed to be suitable for this system [32-34]. The nature of each structure was verified by performing harmonic vibrational frequency calculations. Intrinsic reaction coordinate (IRC) calculations were examined to confirm the right connections among key transition-states and corresponding reactants and products. Harmonic frequency calculations were carried out at the M06-2X/6-31G(d) level to gain zero-point vibrational energy (ZPVE) and thermodynamic corrections at 333 K and 1 atm for each structure in acetonitrile.

The solvation-corrected free energies were obtained at the M06-2X/6-311++G(d,p) level by using integral equation formalism polarizable continuum model (IEFPCM) in Truhlar's "density" solvation model [35-39] on the M06-2X/6-31G(d)-optimized geometries. As an efficient method obtaining bond and lone pair of a molecule from modern ab initio wave functions, NBO procedure was performed with Natural bond orbital (NBO3.1) to characterize electronic properties and bonding orbital interactions [40-42]. The wave function analysis was provided using Multiwfn_3.7_dev package [43] including research on frontier molecular orbital (FMO) and Mayer bond order (MBO).

3 Results and Discussion

The mechanism was explored for $BF_3{\cdot}OEt_2$-facilitated benzannulation and Friedel−Crafts reaction of 2-(phenylethynyl) aniline 1 with 2-(phenylethynyl) benzaldehyde 2 leading to dihydrobenzo[a]indeno[2,1-c]carbazole 3 (Scheme 1). Illustrated by black arrow of Scheme 2, an imine intermediate a is formed through interaction between 2-alkynylaniline 1 and 2-alkynylbenzaldehyde 2 mediated by $BF_3{\cdot}OEt_2$ via initial two steps. Subsequently, the imine group is continuously activated by $BF_3{\cdot}OEt_2$ as corresponding Lewis acid, which undergoes nucleophilic attack by alkyne group of 1 facilitating the formation of alkenyl carbocation intermediate c and five-membered ring. Then c is further attacked by alkyne group of 2 yielding another alkenyl carbocation d and novel six-membered ring. Consecutively, an intramolecular Friedel−Crafts reaction ensues resulting in the formation of intermediate e, the aromatization of which gives rise to neutral intermediate f and the second five-membered ring. Finally, the desired product dihydrobenzo[a]indeno[2,1-c]carbazole 3 is obtained via significant [1,5-H shift] within intermediate f. The schematic structures of optimized TSs in Scheme 2 were listed by Figure 1. The activation energy was shown in Table 1 for all steps. Supplementary Table S1, Table S2 provided the relative energies of all stationary points. According to experiment, the Gibbs free energies in acetonitrile solution phase are discussed here.

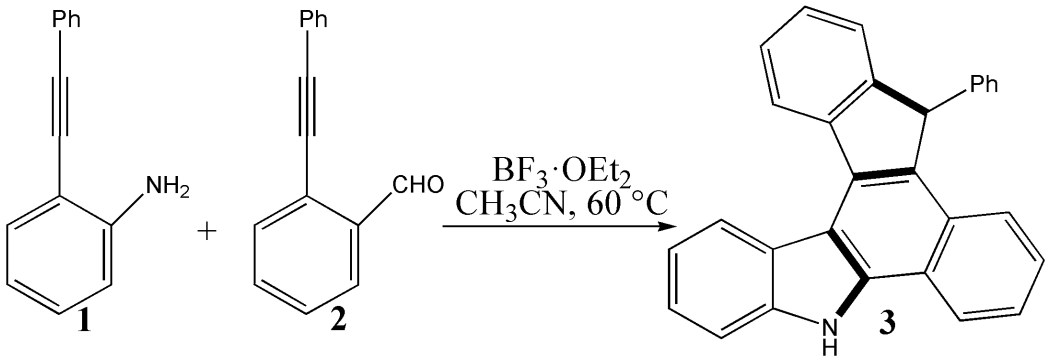

Scheme 1 $BF_3{\cdot}OEt_2$-facilitated benzannulation and Friedel−Crafts reaction of 2-(phenylethynyl)aniline **1** with 2-(phenylethynyl)benzaldehyde **2** leading to dihydrobenzo[a]indeno[2,1-c]carbazole **3**.

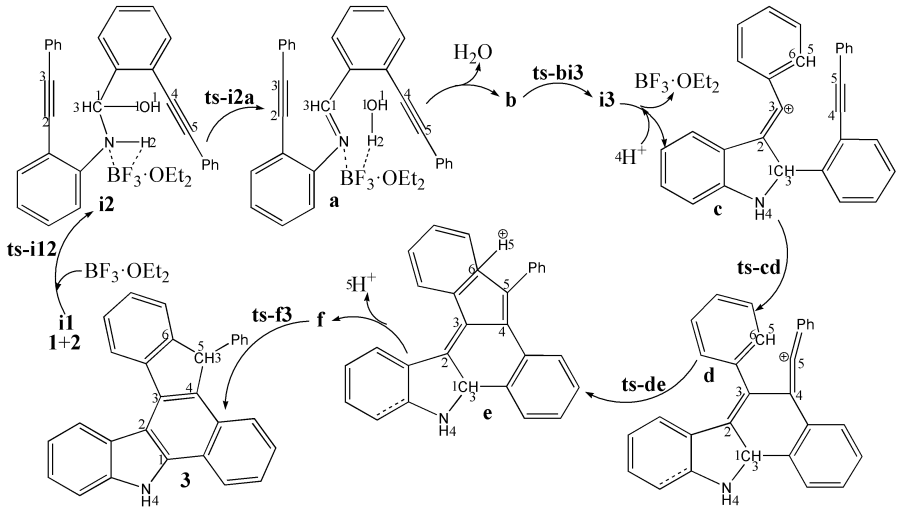

Scheme 2: Proposed reaction mechanism of $BF_3{\cdot}OEt_2$-facilitated benzannulation and Friedel–Crafts reaction of **1** with **2** leading to **3**. TS is named according to the two intermediates it connects.

TS	$\Delta G^{\neq}_{gas}$	$\Delta G^{\neq}_{sol}$
ts-i12	18.5	16.7
ts-i2a	28.8	25.1
ts-bi3	20.1	13.6
ts-cd	9.4	9.2
ts-de	6.6	8.5
ts-f3	30.5	28.1
n-tsi12	28.6	25.3
n-tsi2a	31.6	28.4
n-tsbi3	26.9	21.1

Table 1: The activation energy (in kcal mol^{-1}) of all reactions in gas and solvent

(a)

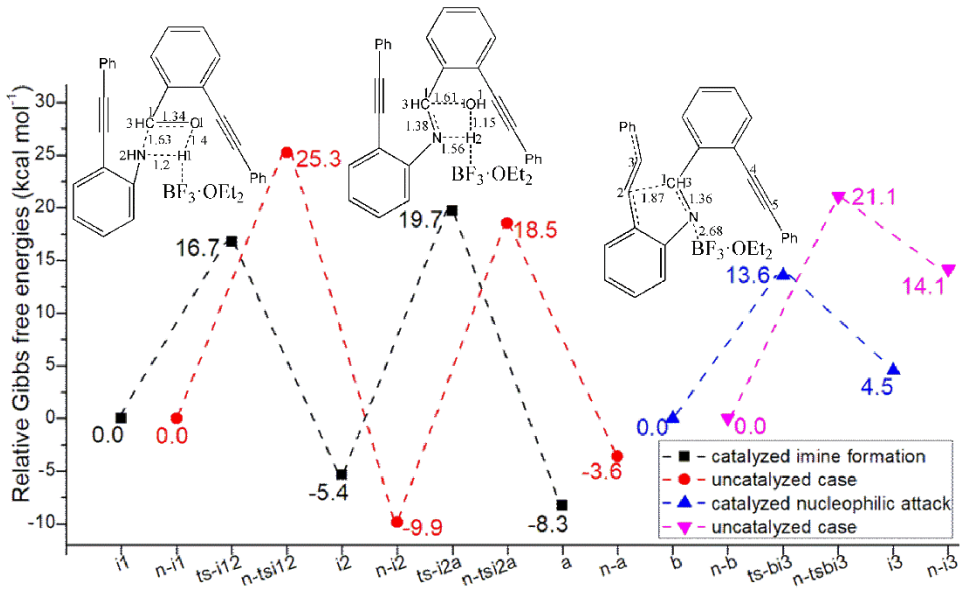

(b)

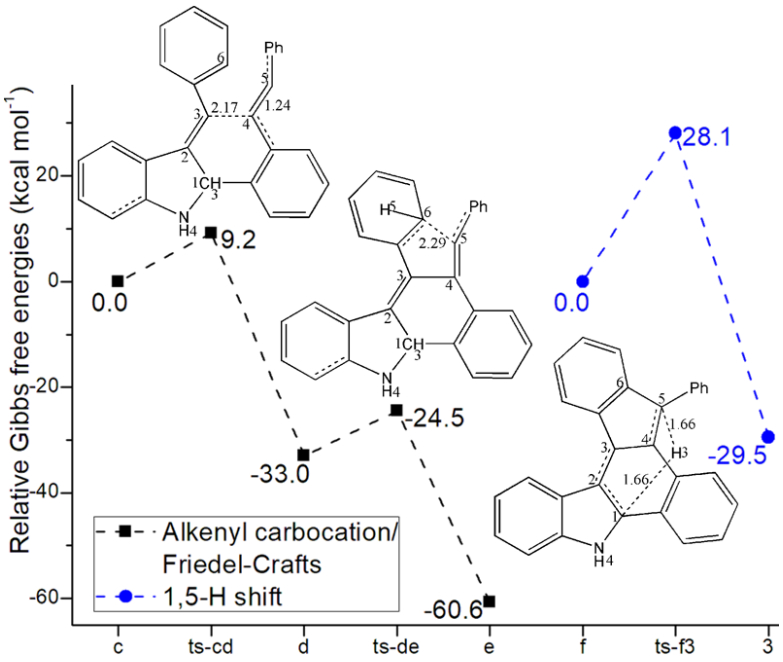

Figure 1: Relative Gibbs free energy profile in solvent phase starting from complex (a) **i1**, **n-i1**, **b**, **n-b** (b) **c**, **f** (Bond lengths of optimized TSs in Å).

Species	ΔG_{gas}	$\Delta G_{sol(CH3CN)}$
1+2+LA	0.00	0.00
i1	-18.98	-12.10
ts-i12	-0.47	4.64
i2	-21.78	-17.49
ts-i2a	7.00	7.58
a	-19.85	-20.36
1+2+LA-H2O	0.00	0.00
b	-6.17	-2.55
ts-bi3	13.96	11.04
i3	0.34	1.98
1+2-H2O+H	0.00	0.00
c	7.25	1.60
ts-cd	16.67	10.76
d	-23.55	-31.39
ts-de	-16.96	-22.90
e	-44.87	-59.02
1+2-H2O	0.00	0.00
f	-15.05	-28.37
ts-f3	15.41	-0.29
3	-44.09	-57.85
1+2	0.00	0.00
n-i1	-13.81	-7.83
n-tsi12	14.80	17.42
n-i2	-14.20	-17.70
n-tsi2a	17.36	10.71
n-a	-8.06	-11.42
1+2-H2O	0.00	0.00
n-b	-3.48	-3.45
n-tsbi3	23.41	17.63
n-i3	12.56	10.69

Table S1. Calculated relative energies (all in kcal mol^{-1}, relative to isolated species) for the ZPE-corrected Gibbs free energies (ΔG_{gas}), Gibbs free energies for all species in solution phase (ΔG_{sol}) at 333 K by M06-2X/6-311++G(d,p)//M06-2X/6-31G(d) method and difference between absolute energy.

TS	$\Delta G^{\neq}_{gas}$	$\Delta G^{\neq}_{sol}$
ts-i12 (1318i)	18.5	16.7
ts-i2a (1131i)	28.8	25.1
ts-bi3 (308i)	20.1	13.6
ts-cd (386i)	9.4	9.2
ts-de (215i)	6.6	8.5
ts-f3 (1566i)	30.5	28.1
n-tsi12 (1426i)	28.6	25.3
n-tsi2a (1013i)	31.6	28.4
n-tsbi3 (411i)	26.9	21.1

Table S2. The activation energy (local barrier) (in kcal mol^{-1}) of all reactions in the gas, solution phase calculated with M06-2X/6-311++G(d,p)//M06-2X/6-31G(d) method.

	N···C1	N···H1	H1···O1	C1···O1
ts-i12	0.80	0.50	0.22	1.25
	N···C1	N···H2	H2···O1	C1···O1
ts-i2a	1.38	0.18	0.71	0.38
	C2···C1	N···C1		
ts-bi3	0.24	1.12		
	C4···C3	C4···C5		
ts-cd	0.32	1.79		
	C6···C5			
ts-de	0.68			
	C1···H3	H3···C5		
ts-f3	0.41	0.40		

Table S3. Mayer bond order (MBO) of typical TSs

3.1 BF_3·OEt_2-mediated imine formation/nucleophilic attack of alkyne

During initial two steps, BF_3·OEt_2 constantly functions as LA not only accepting lone pair electrons via B-N bond but forming H bond depending on F. The complex between **1**, **2** and BF_3·OEt_2 is denoted as **i1**. The nucleophilic addition of **1** to **2** proceeds via **ts-i12** in step 1 with the activation energy of 16.7 kcal mol^{-1} relative to the starting point **i1** exothermic by -5.4 kcal mol^{-1} producing **i2** (black dash line of Figure 1a). The transition vector contains two parts in concerted modes that is nucleophilic attack of negative N to positive C1 along with cooperated transferring of H1 from N to O1 and carbonyl group C1-O1 stretching from double bond to single one (1.63, 1.2, 1.4, 1.34 Å) (Figure S1a). Obviously, **i2** is stable with formal N-C1 single bond.

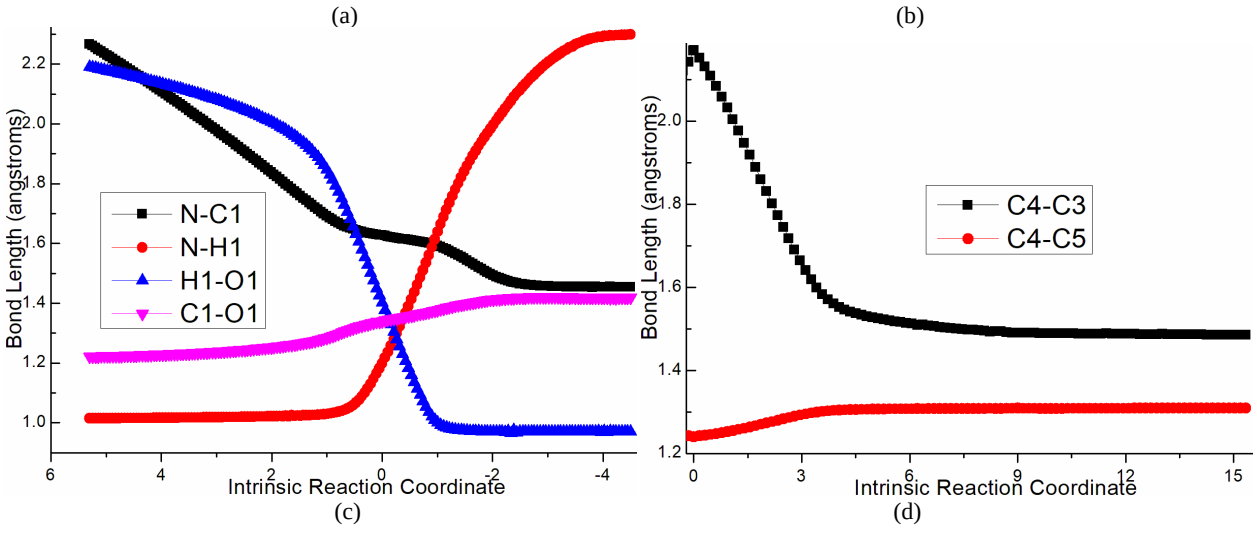

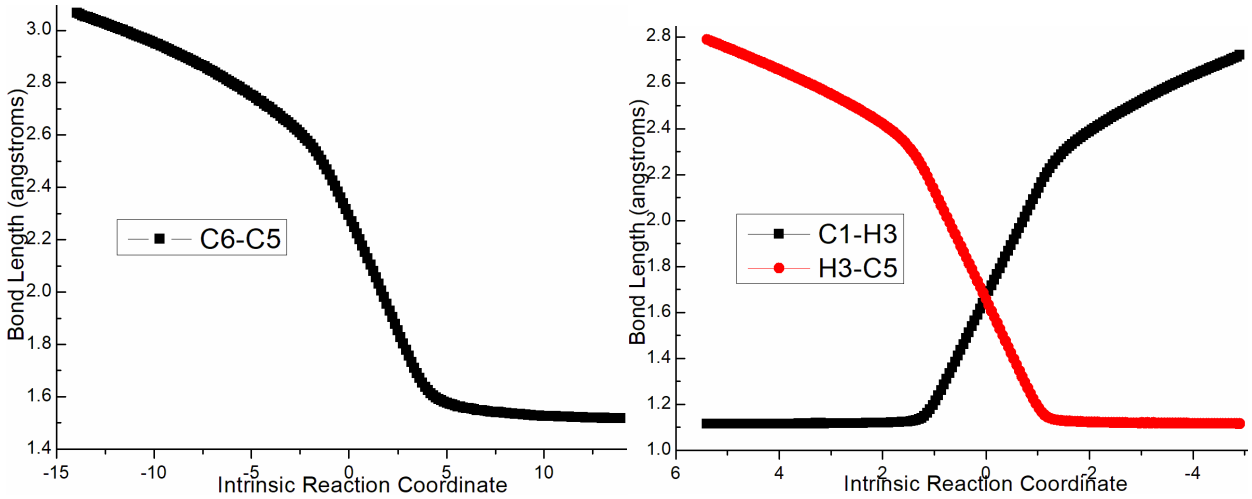

Figure S1. Evolution of bond lengths along the IRC for (a) **ts-i12** (b) **ts-cd** (c) **ts-de** (d) **ts-f3** at M06-2X/6-311++G(d,p) level.

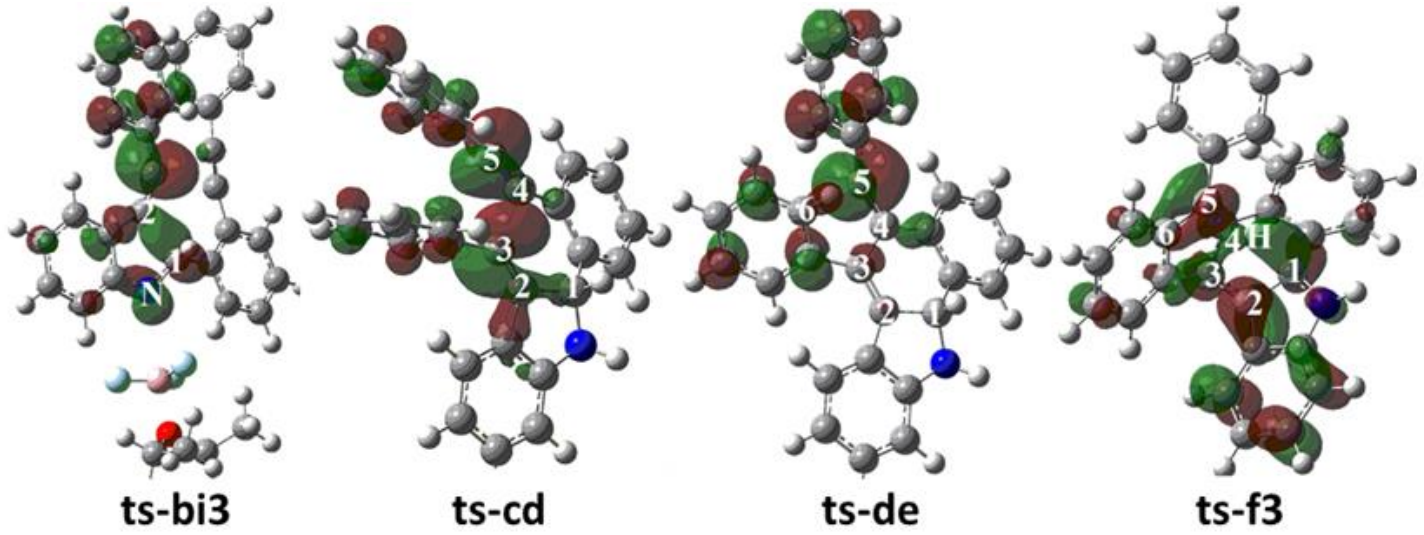

Figure S2. Highest Occupied Molecular Orbital (HOMO) of typical TSs. Different colors are used to identify the phase of the wave functions.

Then mediated by $BF_3{\cdot}OEt_2$, the dehydration process occurs via **ts-i2a** as step 2 with activation energy of 25.1 kcal mol^{-1} exothermic by -8.3 kcal mol^{-1} giving intermediate **a**. The transition vector includes another H2 on N moving to O1 forming water molecule H1-O1-H2 as well as the consquent breaking of C1-O1 single bond, further shortening of N-C1 from single to double (1.56, 1.15, 1.61, 1.38 Å). Both N and C1 turn to be sp2 hybrid in resultant stable **a** with typical imine structure.

Subsequently, after the removal of water, the imine group N-C1 is continuously activated by $BF_3{\cdot}OEt_2$ via B-N interaction in the similar intermediate **b**, which is taken as new starting point initiating nucleophilic attack from alkyne group of **1**. This step 3 takes place via **ts-bi3** with activation energy of 13.6 kcal mol^{-1} affording **i3** endothermic by 4.5 kcal mol^{-1} (blue dash line of Figure 1a). According to the transition vector, as the negative alkyne C2 approaches positive C1, the imine C1-N double bond is elongated promoting π electron focusing on N and further cleavage of B-N bond (1.87, 1.36, 2.68 Å). Hence $BF_3{\cdot}OEt_2$ is leaving from then on and the role of LA is ended in the following process. Once C2-C1 is formed, the first five-membered ring is obtained in **i3**.

3.2 Alkenyl carbocation formatiom/intramolecular Friedel−Crafts/1,5-H shift

An additional proton H4 bonded to negative N facilitates the formation of alkenyl carbocation intermediate **c** with positive charge on alkyne C3. This makes the next two steps from starting point **c** fairly easy. In step 4 **c** is further attacked by alkyne group of **2** via **ts-cd** with activation energy of 9.2 kcal mol^{-1} exothermic by -33.0 kcal mol^{-1} delivering intermediate

d (black dash line of Figure 1b). The transition vector corresponds to the approaching of negative C4 to positive C3 and C4-C5 tripple bond is weakened to double one (2.17, 1.24 Å) (Figure S1b). When C4-C3 single bond is completed, the stable **d** is yielded as the second alkenyl carbocation with novel six-membered ring. In addition, alkyne of **2** becomes accumulated diene with positive charge shifting to C5 ready for the vital Friedel−Crafts reaction closely afterwards.

The intramolecular Friedel−Crafts reaction happens via **ts-de** in step 5 with activation energy of 8.5 kcal mol^{-1} exothermic by -60.6 kcal mol^{-1} generating intermediate **e** rather stable. The transition vector reveals remarkable attack from sp2 hybrid C6 of phenyl to positive C5 (2.29 Å) (Figure S1c). The resulting **e** is characterized by C6-C5 single bond, the second new five-membered ring and sp3 hybrid C6 with positively charged H5. Consecutively, the aromatization of **e** gives rise to neutral intermediate **f** wihtout H5 to accomplish the last step.

Finally, the significant [1,5-H shift] proceeds via **ts-f3** in step 6 with activation energy of 28.1 kcal mol^{-1} relative to **f** yielding the desired product dihydrobenzo[a]indeno[2,1-c]carbazole **3** exothermic by -29.5 kcal mol^{-1} (blue dash line of Figure 1b). The detailed atomic motion is illustrated according to the transition vector about proton H3 transfer from C1 to C5 (1.66, 1.66 Å) (Figure S1d). Evidently, the energy of **ts-f3** is elevated owing to the tension caused by great structure bending required by long-distance shifting. Therefore, 1,5-H shift of step 6 is determined to be rate-limiting for the whole process.

To highlight the idea of feasibility for changes in electron density and not molecular orbital interactions are responsible of the reactivity of organic molecules, quantum chemical tool Multiwfn was applied to analyze of electron density such as MBO results of bonding atoms and contribution of atomic orbital to HOMO of typical TSs (Table S3, Figure S2). These results all confirm the above analysis.

3.3 Comparison with uncatalyzed case

The reaction without $BF_3{\cdot}OEt_2$ are also explored to investigate the promotion of LA. The complex between **1**, **2** is denoted as **n-i1**. The nucleophilic addition of **1** to **2** proceeds via **n-tsi12** in step 1 with the activation energy of 25.3 kcal mol^{-1} exothermic by -9.9 kcal mol^{-1} producing **n-i2**. The next dehydration occurs via **n-tsi2a** as step 2 with activation energy of 28.4 kcal mol^{-1} exothermic by -3.6 kcal mol^{-1} giving **n-a** also with typical imine structure of N-C1 double bond the same as that of **a** (red dash line of Figure 1a). From **n-b**, the nucleophilic attack from alkyne group of **1** takes place via **n-tsbi3** in step 3 with activation energy of 21.1 kcal mol^{-1} affording **n-i3** endothermic by 14.1 kcal mol^{-1} (magenta dash line of Figure 1a).

From kinetics, the barries of previous three steps are all increased for uncatalyzed process compared with $BF_3{\cdot}OEt_2$-facilitated case. Furthermore, the relative energy of most stationary points are comparatively high and is not advantageous from the perspective of entire potential energy surface. The catalytic effect of $BF_3{\cdot}OEt_2$ as LA was fully confirmed from two aspects of lowering activation energy and relative energies.

4 Conclusions

Our DFT calculations provide the first theoretical investigation on $BF_3{\cdot}OEt_2$-facilitated benzannulation and Friedel−Crafts reaction of 2-(phenylethynyl)aniline with 2-(phenylethynyl)benzaldehyde. An imine structure is formed mediated by $BF_3{\cdot}OEt_2$ constantly functioning as LA via initial two steps. The subsequent nucleophilic attack from alkyne group of 2-(phenylethynyl)aniline forms the first alkenyl carbocation and five-membered ring continuously under the influence of $BF_3{\cdot}OEt_2$. With additional proton, the second alkenyl carbocation is given by attack from alkyne group of 2-(phenylethynyl)benzaldehyde together with novel six-membered ring**.** Then an intramolecular Friedel−Crafts reaction and aromatization give rise to the second five-membered ring. The desired product dihydrobenzo[a]indeno[2,1-c]carbazole is obtained via 1,5-H shift, which is determined to be rate-limiting with higher barrier than other five steps owing to the tension resulting from great structure bending required by long-distance shifting. The catalytic effect of $BF_3{\cdot}OEt_2$ as LA is confirmed from both lowering activation energy and relative energies for previous three steps. The positive solvation effect is suggested by decreased absolute and activation energies in acetonitrile solution compared with in gas. These results are supported by Multiwfn analysis on FMO composition of specific TSs, and MBO value of vital bonding, breaking.

Electronic Supplementary Material

Supplementary data available: [Computation information and cartesian coordinates of stationary points; Calculated relative energies for the ZPE-corrected Gibbs free energies (ΔG_{gas}), and Gibbs free energies (ΔG_{sol}) for all species in solution phase at 333 K.

Author contributions: Conceptualization, Nan Lu; Methodology, Nan Lu; Software, Nan Lu; Validation, Nan Lu; Formal Analysis, Nan Lu; Investigation, Nan Lu; Resources, Nan Lu; Data Curation, Nan Lu; Writing-Original Draft Preparation, Nan Lu; Writing-Review & Editing, Nan Lu; Visualization, Nan Lu; Supervision, Chengxia Miao; Project Administration, Chengxia Miao; Funding Acquisition, Chengxia Miao. All authors have read and agreed to the published version of the manuscript.

Funding: This work was supported by National Natural Science Foundation of China (21972079) and Key Laboratory of Agricultural Film Application of Ministry of Agriculture and Rural Affairs, P.R. China.

Conflict of interest: The authors declare no conflict of interest.

References

1. Głuszyńska, A. (2015). Biological Potential of Carbazole Derivatives. *Eur. J. Med. Chem*. 94, 405−426.
2. Li, J.; Grimsdale, A. C. (2010). Carbazole-Based Polymers for Organic Photovoltaic Devices. *Chem*. Soc. Rev. 39, 2399−2410.
3. Liu, D.; Huang, J.; Fu, Z.; Huang, W. (2019). Direct Construction of Carbazoles from 2-Methyl-indole-3-carbaldehydes and Enals. *Green Chem*. 21, 968−972.
4. Singh, S.; Samineni, R.; Pabbaraja, S.; Mehta, G.(2019). A General Carbazole Synthesis via Stitching of Indole−Ynones with Nitromethanes: Application to Total Synthesis of Carbazomycin A, Calothrixin B, and Staurosporinone. Org. Lett. 21, 3372−3376.
5. Gérardin, B.; Traboulsi, I.; Pal, S.; Lebunetelle, G.; Ramondenc, Y. et al. (2022). Direct Synthesis of Benzo [c] Carbazoles by Pd-Catalyzed C−H [4+2] Annulation of 3-Arylindoles with External 1, 3-Dienes. Org. Lett. 24, 8164−8169.
6. Zou, Q.; Tao, F.; Wu, H.; William, W.Y.; Li, T. et al. (2019). A new Carbazole-Based Colorimetric and Fluorescent Sensor with Aggregation Induced Emission for Detection of Cyanide Anion. *Dyes Pigm*. 164, 165−173.
7. Christopher Leslee, D. B.; Karuppannan, S.; Kothottil, M. M. (2021). Carbazole-Hydrazinobenzothiazole a Selective Turn on Fluorescent Sensor for Hg2+ Ions−Its Protein Binding and Electrochemical Application Studies. *J. Photochem. Photobiol*. 415,No.113303.
8. Chen, S.; Li, Y.; Ni, P.; Huang, H.; Deng, G. J. (2016). Indole-to-Carbazole Strategy for the Synthesis of Substituted Carbazoles under Metal-Free Conditions. Org. Lett. 18, 5384−5387.
9. Georgiades, S. N.; Nicolaou, P. G. (2019). Recent Advances in Carbazole Syntheses. Adv. Heterocycl. Chem., 129, 1−88.
10. Wang, Y. Q.; Li, X. H.; He, Q.; Chen, Y.; Xie, Y. Y. et al.

(2011). Design, Synthesis and Biological Evaluation of Substituted 11H-Benzo[a]carbazole-5-carboxamides as Novel Anti-tumor Agents. *Eur. J. Med. Chem*. 46, 5878−5884.

11. Paramasivam, M.; Chitumalla, R. K.; Singh, S. P.; Islam, A.; Han, L. et al. (2015). Tuning the Photovoltaic Performance of Benzocarbazole-Based Sensitizers for Dye-Sensitized Solar Cells: A Joint Experimental and Theoretical Study of the Influence of π-Spacers. *J. Phys. Chem*. C, 119, 17053−17064.
12. Ivaniuk, K.; Cherpak, V.; Stakhira, P.; Hotra, Z.; Minaev, B. et al. (2016). Highly Luminous Sky-Blue Organic Light-Emitting Diodes Based on the Bis [(1,2)(5,6)] indoloanthracene Emissive Layer. *J. Phys. Chem*. C, 120, 6206−6217.
13. Ghanbari, M.; Kianmehr, E.; Karimi Behzad, S.; Ng, S. W. (2016). Direct Synthesis of Benzo [a] Carbazoles by Palladium-Catalyzed Domino Reactions: Synthesis and Photophysical Properties of Diverse Benzo[a]carbazoles. *J. Iran. Chem*. Soc. 13, 7−18.
14. Kuo, C. W.; Konala, A.; Lin, L.; Chiang, T. T.; Huang, C. Y.; Yang, T.H. et al. (2016). Synthesis of Benzo [a] carbazole Derivatives from 3-Ethylindoles by Exploiting the Dual Character of Benzoquinone as an Oxidizing Agent and Dienophile. Chem. Commun. 52, 7870−7873.
15. Jeon, J.; Cheon, C.-H. (2019). Synthesis of Benzo[a]carbazoles via Cyanide-Catalyzed Imino-Stetter Reaction/Friedel−Crafts Reaction Sequence. Org. *Chem. Front*. 6, 456−467.
16. Yuan, Y.; Guo, X.; Zhang, X.; Li, B.; Huang, Q. (2020). Access to 5 H-Benzo[a]carbazol-6-ols and Benzo [6, 7] Cyclohepta [1, 2-b]indol-6-ols via Rhodium-Catalyzed C−H Activation/Carbenoid Insertion/Aldol-Type Cyclization. *Org. Chem*. Front. 7, 3146−3159.
17. Borthakur, U.; Borah, M.; Deka, M. J.; Saikia, A. K. (2016). Synthesis of Tetrahydro-1H-indeno[1,2-b]pyridine via Cascade Cyclization and Friedel-Crafts Reaction. *J. Org. Chem*. 81, 8736−8743.
18. Luo, Z.; Pan, Y.; Yao, Z.; Yang, J.; Zhang, X. et al. (2021). H. BF3·Et2O as a Metal-Free Catalyst for Direct Reductive Amination of Aldehydes with Amines Using Formic Acid as a Reductant. *Green Chem*. 23, 5205−5211.
19. Peng, X.; Zhu, L.; Hou, Y.; Pang, Y.; Li, Y. et al. (2017). Access to Benzo [a] carbazoles and Indeno[1,2-c] Quinolines by a Gold (I)-Catalyzed Tunable Domino Cyclization of Difunctional 1, 2-Diphenylethynes. Org. Lett. 19, 3402−3405.
20. Li, B.; Shen, N.; Wang, K.; Fan, X.; Zhang, X. (2022). Rh (III)-Catalyzed Reaction of 2-Aryl-3-acyl-1H-indoles with A-Diazo Carbonyl Compounds: Synthesis of 5-Carbonyl Substituted Benzo[a]carbazoles via [5+1] Annulation. Asian *J. Org. Chem*. 11, No. e202100710.
21. Biswas, S.; Porashar, B.; Arandhara, P. J.; Saikia, A. K.(2021). Synthesis of Pyrimido[2,1-a]Isoindolone and Isoindolo[2,1-a]-Quinazolinone via Intramolecular Aza-Prins Type Reaction. Chem. Commun. 57, 11701−11704.
22. Biswas, S.; Shit, S.; Behera, B.K.; Sahu, A.K.; Saikia, A.K. (2023). Leveraging cascade alkynyl Prins cyclization towards the stereoselective synthesis of spiro-furan quinazolinone scaffolds. Chem. Commun. 59, 14301−14304.
23. Porashar, B.; Biswas, S.; Sahu, A. K.; Chutia, A.; Saikia, A. (2022). Temperature Tunable Synthesis of Tetrahydro-4H-pyrrolo[3,2-c]quinolin-4-ones and Dihydro-1H-benzo[b]azepines from 2-Aminobenzonitriles and Donor−Acceptor Cyclopropanes. Org. Lett. 24, 9038−9042.
24. Chutia, A.; Arandhara, P.J.; Behera, B.K.; Pradhan, A.; Saikia, A.K. (2024). Synthesis of Benzodioxepinones and Benzoxazepinones via Tandem Oxidation and Iodolactonization of 2-O/N-Tethered Alkenyl Benzaldehyde Mediated by CuI/TBHP. ACS Omega, 9, 14217−14232.
25. https://pubs.acs.org/doi/abs/10.1021/acs.joc.4c01245
26. Frisch, M. J.; Trucks, G. W.; Schlegel, H. B. et al. (2010). Gaussian 09 (Revision B.01), Gaussian, Inc., Wallingford, CT.
27. Stephens, P. J.; Devlin, F. J.; Chabalowski, C. F.; Frisch, M. (1994). J. Ab initio Calculation of Vibrational Absorption and Circular Dichroism Spectra Using Density Functional Force Fields, *J. Phys. Chem*. 98, 11623-11627.
28. Becke, A. D. (1996). Density-functional thermochemistry. IV. A new dynamical correlation functional and implications for exact-exchange mixing. *J. Chem.* Phys. 104, 1040-1046.
29. Lee, C. T.; Yang,W. T.; Parr, R. G. (1988). Development of the Colle-Salvetti correlation-energy formula into a functional of the electron density. Phys. Rev. B .37, 785-789.
30. Li, X.; Kong, X.; Yang, S.; Meng, M.; Zhan, X. et al. (2019). Bifunctional Thiourea-Catalyzed Asymmetric Inverse-Electron-Demand Diels-Alder Reaction of Allyl Ketones and Vinyl 1,2-Diketones via Dienolate Intermediate, Org. Lett. 21, 1979-1983.
31. Krenske, E. H.; Houk, K. N.; Harmata, M. (2015). Computational Analysis of the Stereochemical Outcome in the Imidazolidinone-Catalyzed Enantioselective (4 + 3)-Cycloaddition Reaction, *J. Org. Chem*. 80, 744-750.
32. Lv, H.; Han, F.; Wang, N.; Lu, N.; Song, Z. et al. (2022). Ionic Liquid Catalyzed C-C Bond Formation for the Synthesis of Polysubstituted Olefins. *Eur. J. Org*. Chem. e202201222.
33. Zhuang, H.; Lu, N.; Ji, N.; Han, F.; Miao, C. (2021). Bu4NHSO4-Catalyzed Direct N-Allylation of Pyrazole and its Derivatives with Allylic Alcohols in Water: A Metal-free, Recyclable and Sustainable System. Advanced Synthesis & Catalysis, 363, 5461-5472.
34. Lu, N.; Liang, H.; Qian, P.; Lan, X.; Miao, C. (2020). Theoretical investigation on the mechanism and enantioselectivity of organocatalytic asymmetric Povarov reactions of anilines and aldehydes. *Int. J. Quantum Chem.* 120, e26574.
35. Tapia, O. (1992). Solvent effect theories: Quantum and classical formalisms and their applications in chemistry and biochemistry. *J. Math. Chem*. 10, 139-181.
36. Tomasi, J.; Persico, M.(1994). Molecular Interactions in Solution: An Overview of Methods Based on Continuous Distributions of the Solvent. Chem. Rev. 94, 2027-2094.
37. Simkin, B. Y.; Sheikhet, I. (1995). Quantum Chemical and Statistical Theory of Solutions—A Computational Approach, Ellis Horwood, London.
38. Tomasi, J.; Mennucci, B.; Cammi, R. (2005). Quantum Mechanical Continuum Solvation Models. Chem. Rev. , 105,

2999-3093.

39. Marenich, A. V.; Cramer, C. J.; Truhlar, D. G. (2009). Universal Solvation Model Based on Solute Electron Density and on a Continuum Model of the Solvent Defined by the Bulk Dielectric Constant and Atomic Surface Tensions. *J. Phys. Chem*. B, 113, 6378–6396.
40. Reed, A. E.; Weinstock, R. B.; Weinhold, F. (1985). Natural population analysis. *J. Chem. Phys*. 1985, 83, 735-746.
41. Reed, A. E.; Curtiss, L. A.; Weinhold, F. (1988). Intermolecular interactions from a natural bond orbital donor-acceptor view point. *Chem*. Rev. 88, 899-926.
42. Foresman, J. B.; Frisch, A. (1996). Exploring Chemistry with Electronic Structure Methods, 2nd ed., Gaussian, Inc., Pittsburgh.
43. Lu, T.; Chen, F. (2012). Multiwfn: A multifunctional wavefunction analyzer. *J. Comput*. Chem., 33, 580-592.

Center Number	Atomic Number	Atomic Type	Coordinates (Angstroms) X	Y	Z
1	6	0	-3.654507	1.034769	-3.671443
2	6	0	-3.856272	-0.017497	-2.782351
3	6	0	-3.176378	-0.045404	-1.569897
4	6	0	-2.291190	0.975155	-1.228699
5	6	0	-2.080142	2.044264	-2.121210
6	6	0	-2.773060	2.055043	-3.340277
7	7	0	-1.663401	0.937936	0.061623
8	6	0	-0.109572	1.200408	0.466343
9	6	0	-1.137500	3.066944	-1.810334
10	6	0	0.610936	-0.116335	0.629562
11	6	0	1.469685	-0.590265	-0.380669
12	6	0	1.695650	0.211004	-1.552145
13	6	0	-0.229388	3.813052	-1.517317
14	6	0	0.469320	-0.840542	1.809021
15	6	0	1.142998	-2.045167	1.982307
16	6	0	1.972003	-2.533045	0.971046
17	6	0	2.141892	-1.807141	-0.200914
18	6	0	1.870527	0.988183	-2.465487
19	6	0	0.917326	4.545613	-1.080673
20	6	0	2.073184	1.954649	-3.505799
21	6	0	1.013653	2.318018	-4.349019
22	6	0	1.202643	3.284364	-5.329981
23	6	0	2.445360	3.898715	-5.480580
24	6	0	3.501341	3.542171	-4.644211
25	6	0	3.320164	2.575244	-3.661888
26	6	0	2.446716	5.112190	0.693899
27	6	0	3.206441	5.859982	-0.204424
28	6	0	2.829876	5.940052	-1.544471
29	6	0	1.688069	5.284923	-1.987599
30	1	0	-4.183865	1.062908	-4.618339
31	1	0	-4.545013	-0.819442	-3.027645
32	1	0	-3.345153	-0.855217	-0.866858
33	1	0	-2.601781	2.884453	-4.019620
34	1	0	-0.161726	-0.416489	2.585842
35	1	0	1.045925	-2.593758	2.915754
36	1	0	2.505297	-3.469382	1.105962
37	1	0	2.805656	-2.163800	-0.981972
38	1	0	0.307234	1.751178	-0.381081
39	1	0	0.047927	1.839295	-4.218685
40	1	0	0.376406	3.560301	-5.978378
41	1	0	2.589391	4.653970	-6.247275
42	1	0	4.469554	4.020956	-4.754646
43	1	0	4.133375	2.301910	-2.997615
44	1	0	2.750454	5.039391	1.733674
45	1	0	4.099703	6.374476	0.137764
46	1	0	3.431193	6.509297	-2.247086

47	1	0	1.394127	5.318551	-3.032889
48	6	0	1.302759	4.447754	0.266537
49	1	0	0.713306	3.831302	0.945500
50	5	0	-3.410383	-2.119948	1.870509
51	9	0	-3.509105	-1.525351	3.091269
52	9	0	-2.287918	-1.750037	1.161414
53	9	0	-4.560240	-2.104176	1.142486
54	8	0	-3.132034	-3.688768	2.132820
55	6	0	-4.264491	-4.553042	2.399837
56	1	0	-5.001070	-4.252155	1.656998
57	1	0	-3.930448	-5.570507	2.179298
58	6	0	-4.804776	-4.409776	3.808868
59	1	0	-5.739919	-4.971554	3.888042
60	1	0	-4.113192	-4.807403	4.554864
61	1	0	-5.006248	-3.359732	4.033005
62	6	0	-1.827450	-4.065493	2.649380
63	1	0	-1.119486	-3.711718	1.897242
64	1	0	-1.819739	-5.158857	2.664289
65	6	0	-1.514607	-3.478046	4.011782
66	1	0	-2.267064	-3.743104	4.756397
67	1	0	-0.552862	-3.883600	4.341418
68	1	0	-1.443518	-2.389758	3.976060
69	8	0	-0.405729	1.901034	1.569166
70	1	0	-1.639382	1.780851	0.913715
71	1	0	-1.927156	0.067332	0.536272

Optimized Cartesian coordinates for **ts-i2a**

Center Number	Atomic Number	Atomic Type	Coordinates (Angstroms) X	Y	Z
1	6	0	-0.465167	-2.598992	3.787843
2	6	0	0.862569	-2.672356	3.359238
3	6	0	1.319785	-1.859782	2.333773
4	6	0	0.485746	-0.923549	1.694741
5	6	0	-0.859009	-0.838269	2.159329
6	6	0	-1.312952	-1.684048	3.184465
7	7	0	1.029756	-0.137590	0.696047
8	6	0	0.355833	-0.018009	-0.507469
9	6	0	-1.746708	0.144897	1.626841
10	6	0	0.640636	-1.072065	-1.553027
11	6	0	-0.409490	-1.838234	-2.084196
12	6	0	-1.767106	-1.601497	-1.683169
13	6	0	-2.488973	0.977797	1.148669
14	6	0	1.959331	-1.377756	-1.893699
15	6	0	2.241069	-2.390280	-2.801056
16	6	0	1.198531	-3.140081	-3.347596
17	6	0	-0.113506	-2.876088	-2.981714
18	6	0	-2.901663	-1.425849	-1.297830
19	6	0	-3.324243	1.952824	0.519443
20	6	0	-4.237880	-1.277128	-0.798689
21	6	0	-4.557423	-1.777058	0.472525
22	6	0	-5.857080	-1.672329	0.953171
23	6	0	-6.845648	-1.065130	0.178579
24	6	0	-6.528238	-0.555197	-1.078219
25	6	0	-5.230778	-0.658435	-1.567660
26	6	0	-5.522025	2.803611	-0.029828
27	6	0	-4.946923	3.838710	-0.764139
28	6	0	-3.559239	3.930404	-0.859682
29	6	0	-2.750830	2.996302	-0.224444
30	1	0	-0.828170	-3.241812	4.583119
31	1	0	1.541345	-3.387401	3.816444
32	1	0	2.332904	-1.942489	1.957296
33	1	0	-2.344313	-1.585304	3.513189
34	1	0	2.769745	-0.840908	-1.402915
35	1	0	3.270789	-2.612968	-3.063889

36	1	0	1.412208	-3.943711	-4.045259
37	1	0	-0.929692	-3.469945	-3.379897
38	1	0	-0.696882	0.283286	-0.524009
39	1	0	-3.775444	-2.237369	1.068878
40	1	0	-6.100122	-2.064134	1.936151
41	1	0	-7.860392	-0.987023	0.557174
42	1	0	-7.292278	-0.071884	-1.679563
43	1	0	-4.973649	-0.259265	-2.543405
44	1	0	-6.602654	2.719538	0.041881
45	1	0	-5.576424	4.570226	-1.261759
46	1	0	-3.104788	4.734556	-1.430805
47	1	0	-1.668749	3.059547	-0.294882
48	6	0	-4.720520	1.865823	0.609204
49	1	0	-5.164267	1.047103	1.167966
50	5	0	3.821202	0.406330	0.924330
51	9	0	3.554703	1.219637	-0.134625
52	9	0	3.965218	-0.897127	0.704750
53	9	0	3.598857	0.890306	2.132217
54	8	0	5.838156	0.739162	0.900281
55	6	0	6.330580	2.042408	1.199757
56	1	0	5.680579	2.409967	1.996361
57	1	0	7.342622	1.939438	1.612295
58	6	0	6.325499	2.991149	0.012304
59	1	0	6.611918	3.993343	0.344664
60	1	0	7.038880	2.679163	-0.756256
61	1	0	5.327784	3.042256	-0.429727
62	6	0	6.634860	-0.055893	0.020630
63	1	0	6.631217	-1.065651	0.438500
64	1	0	7.665226	0.319531	0.056750
65	6	0	6.106255	-0.071912	-1.404448
66	1	0	6.114771	0.924865	-1.851770
67	1	0	6.725375	-0.733627	-2.017526
68	1	0	5.081689	-0.447120	-1.417589
69	8	0	1.075946	1.320622	-1.023475
70	1	0	1.717186	1.075920	-1.720558
71	1	0	1.597173	1.367729	-0.164213

Optimized Cartesian coordinates for **ts-bi3**

Center Number	Atomic Number	Atomic Type	Coordinates (Angstroms) X	Y	Z
1	6	0	-0.554269	4.752196	-0.297864
2	6	0	-1.908562	4.407338	-0.495401
3	6	0	-2.349236	3.102210	-0.449874
4	6	0	-1.415598	2.068011	-0.179746
5	6	0	-0.053071	2.434613	0.019799
6	6	0	0.374770	3.765509	-0.030609
7	7	0	-1.638955	0.737511	-0.203332
8	6	0	-0.647073	0.092599	0.461025
9	6	0	0.782508	1.272170	0.209330
10	6	0	-0.557913	-1.398933	0.234638
11	6	0	0.622164	-2.159363	0.091828
12	6	0	1.985627	-1.693529	0.060292
13	6	0	1.977584	1.093690	0.584490
14	6	0	-1.779481	-2.088904	0.216847
15	6	0	-1.840951	-3.469502	0.075694
16	6	0	-0.678905	-4.215945	-0.075255
17	6	0	0.536690	-3.558022	-0.071058
18	6	0	3.190234	-1.657236	-0.092012
19	6	0	3.368522	1.374787	0.525575
20	6	0	4.616534	-1.618336	-0.214695
21	6	0	5.432076	-2.073878	0.830721
22	6	0	6.812122	-2.116763	0.674015
23	6	0	7.395918	-1.704893	-0.521918
24	6	0	6.592443	-1.246353	-1.564048

25	6	0	5.212224	-1.203694	-1.415098
26	6	0	5.453136	1.870962	1.655742
27	6	0	6.058863	2.122034	0.425057
28	6	0	5.330151	1.994351	-0.757703
29	6	0	3.992650	1.631744	-0.711920
30	1	0	-0.244510	5.789563	-0.369624
31	1	0	-2.626912	5.198109	-0.694896
32	1	0	-3.394360	2.862884	-0.600984
33	1	0	1.425129	3.998557	0.122452
34	1	0	-2.724402	-1.565358	0.304499
35	1	0	-2.809552	-3.962181	0.074488
36	1	0	-0.716222	-5.294371	-0.193591
37	1	0	1.461465	-4.110887	-0.195279
38	1	0	-0.530829	0.353752	1.522644
39	1	0	4.969105	-2.400732	1.756486
40	1	0	7.434291	-2.474681	1.488610
41	1	0	8.474394	-1.742349	-0.641896
42	1	0	7.042299	-0.925673	-2.498827
43	1	0	4.578062	-0.860369	-2.226827
44	1	0	6.024862	1.969800	2.573477
45	1	0	7.104088	2.412895	0.386427
46	1	0	5.807944	2.181872	-1.714573
47	1	0	3.401087	1.546259	-1.618909
48	6	0	4.123493	1.478439	1.707801
49	1	0	3.641526	1.261242	2.655524
50	5	0	-4.418490	-0.006809	-0.579177
51	9	0	-4.098958	-0.028889	0.742232
52	9	0	-4.014972	-1.052357	-1.332566
53	9	0	-4.458255	1.206652	-1.170855
54	8	0	-6.122228	-0.365756	-0.505919
55	6	0	-6.977643	0.620016	0.095867
56	1	0	-6.532684	1.568447	-0.206016
57	1	0	-7.959417	0.528243	-0.381539
58	6	0	-7.076711	0.506560	1.605833
59	1	0	-7.644832	1.358416	1.990924
60	1	0	-7.598486	-0.405451	1.910318
61	1	0	-6.079870	0.516428	2.051322
62	6	0	-6.524791	-1.742649	-0.405563
63	1	0	-6.287303	-2.184669	-1.374749
64	1	0	-7.612447	-1.748989	-0.276030
65	6	0	-5.821773	-2.492672	0.711568
66	1	0	-5.997708	-2.038057	1.688221
67	1	0	-6.196834	-3.520465	0.732039
68	1	0	-4.745660	-2.522708	0.533421

Optimized Cartesian coordinates for **ts-cd**

Center Number	Atomic Number	Atomic Type	Coordinates (Angstroms) X	Y	Z
1	6	0	-2.834015	-3.869616	0.472279
2	6	0	-4.185623	-3.487949	0.526647
3	6	0	-4.584826	-2.186009	0.268112
4	6	0	-3.600735	-1.253255	-0.060601
5	6	0	-2.248670	-1.620873	-0.097009
6	6	0	-1.858046	-2.942307	0.154729
7	7	0	-3.794694	0.108013	-0.331776
8	6	0	-2.502178	0.660861	-0.751113
9	6	0	-1.476083	-0.414578	-0.404175
10	6	0	-2.228367	2.056118	-0.258291
11	6	0	-0.918300	2.503766	-0.063422
12	6	0	0.244125	1.655003	-0.196657
13	6	0	-0.164925	-0.429872	-0.636247
14	6	0	-3.282822	2.949237	-0.079427
15	6	0	-3.045316	4.269698	0.280444
16	6	0	-1.738243	4.720241	0.464328

17	6	0	-0.680335	3.842480	0.295014
18	6	0	1.472456	1.489875	-0.230026
19	6	0	0.924196	-1.273094	-0.236456
20	6	0	2.839706	1.164315	-0.140199
21	6	0	3.533840	1.431134	1.058637
22	6	0	4.883152	1.135829	1.146187
23	6	0	5.536808	0.539412	0.063757
24	6	0	4.852184	0.254101	-1.117393
25	6	0	3.508697	0.577183	-1.233387
26	6	0	2.691705	-2.807442	-0.878208
27	6	0	3.087620	-2.892817	0.453941
28	6	0	2.407187	-2.177076	1.444565
29	6	0	1.318962	-1.387226	1.111251
30	1	0	-2.560777	-4.896853	0.685555
31	1	0	-4.932989	-4.234108	0.777348
32	1	0	-5.629073	-1.892645	0.300414
33	1	0	-0.812568	-3.229846	0.105706
34	1	0	-4.518970	0.251908	-1.030220
35	1	0	-4.301253	2.594721	-0.198793
36	1	0	-3.880454	4.948654	0.416941
37	1	0	-1.544710	5.751008	0.741019
38	1	0	0.342025	4.175913	0.440066
39	1	0	-2.472604	0.709128	-1.852536
40	1	0	3.003962	1.879196	1.893352
41	1	0	5.427237	1.354628	2.058630
42	1	0	6.591985	0.296647	0.142130
43	1	0	5.370561	-0.208465	-1.950683
44	1	0	2.963323	0.377097	-2.148530
45	1	0	3.218546	-3.368992	-1.642549
46	1	0	3.931573	-3.518307	0.727396
47	1	0	2.721826	-2.252604	2.480115
48	1	0	0.769488	-0.839770	1.871983
49	6	0	1.638110	-1.971735	-1.228748
50	1	0	1.334160	-1.865817	-2.266109

Optimized Cartesian coordinates for **ts-de**

Center Number	Atomic Number	Atomic Type	Coordinates (Angstroms) X	Y	Z
1	6	0	4.908352	-2.146843	0.175866
2	6	0	5.818843	-1.083834	0.069586
3	6	0	5.400579	0.239892	0.071562
4	6	0	4.032957	0.490749	0.179061
5	6	0	3.106284	-0.567508	0.276289
6	6	0	3.549670	-1.895608	0.276322
7	7	0	3.396980	1.731190	0.186345
8	6	0	2.020875	1.508779	0.629962
9	6	0	1.790599	0.036370	0.359752
10	6	0	0.966148	2.411790	0.043012
11	6	0	-0.349328	1.943826	-0.080589
12	6	0	-0.599394	0.498149	0.179605
13	6	0	0.531870	-0.437482	0.231270
14	6	0	1.256708	3.729512	-0.300520
15	6	0	0.253758	4.580132	-0.750348
16	6	0	-1.057662	4.118951	-0.855416
17	6	0	-1.356527	2.803955	-0.529566
18	6	0	-1.819231	-0.015233	0.202376
19	6	0	0.048713	-1.814567	0.029318
20	6	0	-3.219917	-0.020777	0.227905
21	6	0	-3.940487	-0.337474	-0.949265
22	6	0	-5.323180	-0.299563	-0.937314
23	6	0	-5.996095	0.038898	0.241230
24	6	0	-5.297607	0.345076	1.413914
25	6	0	-3.914638	0.311373	1.416534
26	6	0	-1.856906	-3.303545	0.392963

27	6	0	-1.383081	-4.142226	-0.598299
28	6	0	-0.184905	-3.832088	-1.261666
29	6	0	0.528359	-2.678528	-0.958007
30	1	0	5.273852	-3.167439	0.189273
31	1	0	6.879661	-1.300397	-0.008828
32	1	0	6.113654	1.053963	-0.006889
33	1	0	2.845532	-2.713608	0.387160
34	1	0	3.899603	2.478387	0.651592
35	1	0	2.279467	4.086218	-0.228682
36	1	0	0.494471	5.602618	-1.022087
37	1	0	-1.842890	4.779940	-1.206410
38	1	0	-2.372632	2.438020	-0.644512
39	1	0	1.974664	1.623072	1.728611
40	1	0	-3.389569	-0.605940	-1.845102
41	1	0	-5.884004	-0.534175	-1.835302
42	1	0	-7.081581	0.063921	0.246538
43	1	0	-5.839414	0.608432	2.315635
44	1	0	-3.348469	0.550184	2.311505
45	1	0	-2.760746	-3.551017	0.940994
46	1	0	-1.925212	-5.045015	-0.858173
47	1	0	0.172794	-4.486653	-2.050574
48	1	0	1.414324	-2.411863	-1.525799
49	6	0	-1.135480	-2.140828	0.721628
50	1	0	-1.356311	-1.633258	1.659931

Optimized Cartesian coordinates for **ts-f3**

Center Number	Atomic Number	Atomic Type	Coordinates (Angstroms) X	Y	Z
1	6	0	-5.084992	1.096704	0.087819
2	6	0	-5.321714	0.243703	1.178644
3	6	0	-4.378891	-0.684727	1.591277
4	6	0	-3.177385	-0.745487	0.881344
5	6	0	-2.904406	0.130477	-0.196597
6	6	0	-3.883059	1.046294	-0.599388
7	7	0	-2.112318	-1.601342	1.050147
8	6	0	-1.076734	-1.236913	0.191313
9	6	0	-1.576373	-0.184033	-0.672834
10	6	0	-0.122108	-2.195174	-0.375366
11	6	0	0.831834	-1.581166	-1.202674
12	6	0	0.678482	-0.120107	-1.218144
13	6	0	-0.589008	0.506116	-1.403570
14	6	0	-0.078082	-3.568059	-0.139802
15	6	0	0.942759	-4.318496	-0.714941
16	6	0	1.913122	-3.705387	-1.509948
17	6	0	1.865947	-2.334169	-1.748354
18	6	0	1.301527	0.613847	-0.171299
19	6	0	0.700632	1.965584	-0.175541
20	6	0	-0.438227	1.927265	-1.006073
21	6	0	2.639232	0.327671	0.416313
22	6	0	3.708706	1.190886	0.152667
23	6	0	4.975256	0.925789	0.664206
24	6	0	5.189305	-0.205833	1.446320
25	6	0	4.131588	-1.072736	1.710502
26	6	0	2.865548	-0.807706	1.198606
27	6	0	1.062015	3.128582	0.496670
28	6	0	0.287988	4.270657	0.307254
29	6	0	-0.830897	4.240480	-0.528749
30	6	0	-1.212582	3.067950	-1.180149
31	1	0	-5.854773	1.796286	-0.220324
32	1	0	-6.269975	0.303793	1.704155
33	1	0	-4.572043	-1.351735	2.425722
34	1	0	-3.708862	1.689276	-1.454835
35	1	0	-2.013742	-2.249324	1.815771
36	1	0	-0.844104	-4.047295	0.464486

37	1	0	0.981847	-5.390289	-0.545883
38	1	0	2.709305	-4.301345	-1.944750
39	1	0	2.623852	-1.847600	-2.354831
40	1	0	0.149216	-0.221081	0.679161
41	1	0	3.542350	2.067879	-0.467384
42	1	0	5.795771	1.603964	0.449787
43	1	0	6.176561	-0.411456	1.848887
44	1	0	4.292249	-1.958163	2.318210
45	1	0	2.038550	-1.484173	1.401962
46	1	0	1.926173	3.142582	1.155167
47	1	0	0.557532	5.194072	0.810434
48	1	0	-1.411218	5.146310	-0.677201
49	1	0	-2.076449	3.065123	-1.836068

Optimized Cartesian coordinates for **n-tsi12**

Center Number	Atomic Number	Atomic Type	Coordinates (Angstroms) X	Y	Z
1	6	0	-1.951843	2.052916	-4.293075
2	6	0	-2.187994	0.743805	-3.877663
3	6	0	-1.874229	0.359284	-2.578687
4	6	0	-1.314802	1.274286	-1.693041
5	6	0	-1.065533	2.596121	-2.100866
6	6	0	-1.397680	2.969280	-3.411395
7	7	0	-0.992337	0.882478	-0.351115
8	6	0	0.509073	0.845207	0.256653
9	6	0	-0.477339	3.522037	-1.189080
10	6	0	0.961718	-0.590068	0.420965
11	6	0	1.394218	-1.363606	-0.673341
12	6	0	1.390370	-0.792527	-1.986694
13	6	0	0.041497	4.242115	-0.363882
14	6	0	0.949257	-1.148540	1.694300
15	6	0	1.357634	-2.465101	1.892342
16	6	0	1.783809	-3.233393	0.810840
17	6	0	1.802729	-2.687010	-0.467310
18	6	0	1.337246	-0.251514	-3.069528
19	6	0	0.672300	5.077577	0.611773
20	6	0	1.209456	0.431053	-4.320755
21	6	0	0.715554	-0.235630	-5.451156
22	6	0	0.545018	0.450947	-6.646390
23	6	0	0.868658	1.804810	-6.729091
24	6	0	1.368254	2.469862	-5.611574
25	6	0	1.538558	1.790437	-4.411162
26	6	0	1.789029	5.314937	2.734080
27	6	0	1.920548	6.684679	2.512561
28	6	0	1.426699	7.253673	1.339748
29	6	0	0.803251	6.455624	0.389346
30	1	0	-2.182851	2.352537	-5.310093
31	1	0	-2.608669	0.018958	-4.567055
32	1	0	-2.037671	-0.664953	-2.253084
33	1	0	-1.196919	3.988658	-3.724526
34	1	0	0.627487	-0.512640	2.512907
35	1	0	1.348572	-2.891060	2.891093
36	1	0	2.106217	-4.258968	0.962280
37	1	0	2.134583	-3.274234	-1.317544
38	1	0	1.105912	1.373448	-0.507684
39	1	0	0.461419	-1.288256	-5.375066
40	1	0	0.160165	-0.070657	-7.517476
41	1	0	0.736385	2.337741	-7.665806
42	1	0	1.623092	3.523560	-5.672982
43	1	0	1.911853	2.303965	-3.530018
44	1	0	2.174748	4.875180	3.648811
45	1	0	2.408110	7.310852	3.253895
46	1	0	1.528049	8.320636	1.166356
47	1	0	0.413793	6.885978	-0.527924

48	6	0	1.168127	4.502703	1.792039
49	1	0	1.049232	3.430117	1.934861
50	8	0	0.205812	1.505895	1.379838
51	1	0	-0.961134	1.598958	0.614880
52	1	0	-1.454461	0.005786	-0.101140

Optimized Cartesian coordinates for **n-tsi2a**

Center Number	Atomic Number	Atomic Type	Coordinates (Angstroms) X	Y	Z
1	6	0	-0.147508	-2.599269	3.435458
2	6	0	1.150771	-2.680952	2.937474
3	6	0	1.564089	-1.822858	1.926419
4	6	0	0.709494	-0.845959	1.406437
5	6	0	-0.600436	-0.749104	1.922814
6	6	0	-1.010476	-1.639728	2.925592
7	7	0	1.170708	0.050319	0.425075
8	6	0	0.570567	-0.016155	-0.902605
9	6	0	-1.512148	0.266199	1.491801
10	6	0	0.755782	-1.379424	-1.559404
11	6	0	-0.317673	-2.265052	-1.751853
12	6	0	-1.662223	-1.891761	-1.411861
13	6	0	-2.341142	1.090548	1.171874
14	6	0	2.035446	-1.764422	-1.961361
15	6	0	2.264107	-3.010558	-2.531491
16	6	0	1.199975	-3.894104	-2.712694
17	6	0	-0.080578	-3.522738	-2.330342
18	6	0	-2.805436	-1.570307	-1.170806
19	6	0	-3.364892	2.014347	0.784177
20	6	0	-4.149115	-1.139557	-0.912545
21	6	0	-4.630710	-1.057187	0.400224
22	6	0	-5.902607	-0.553051	0.644474
23	6	0	-6.708608	-0.138169	-0.413186
24	6	0	-6.244467	-0.241087	-1.723314
25	6	0	-4.971952	-0.738031	-1.975044
26	6	0	-4.708625	3.038841	-0.945958
27	6	0	-5.439199	3.725111	0.022218
28	6	0	-5.133291	3.557211	1.371070
29	6	0	-4.105206	2.704246	1.754047
30	1	0	-0.482606	-3.272596	4.217311
31	1	0	1.840706	-3.424210	3.325051
32	1	0	2.565991	-1.910516	1.513496
33	1	0	-2.020663	-1.546570	3.312528
34	1	0	2.854800	-1.060918	-1.831789
35	1	0	3.266078	-3.291718	-2.840856
36	1	0	1.368519	-4.870062	-3.156973
37	1	0	-0.919088	-4.195611	-2.477846
38	1	0	-0.497308	0.208602	-0.807158
39	1	0	-3.982889	-1.354713	1.218171
40	1	0	-6.261278	-0.471104	1.665765
41	1	0	-7.698255	0.262968	-0.217507
42	1	0	-6.871454	0.077245	-2.550654
43	1	0	-4.592742	-0.803108	-2.990169
44	1	0	-4.951316	3.157157	-1.997732
45	1	0	-6.246996	4.387302	-0.273951
46	1	0	-5.699746	4.090144	2.128688
47	1	0	-3.866287	2.559945	2.802878
48	6	0	-3.674055	2.191127	-0.571238
49	1	0	-3.109121	1.639968	-1.316812
50	8	0	1.251652	0.981588	-1.632584
51	1	0	0.953505	0.922593	-2.551145
52	1	0	2.180093	-0.017976	0.320379

Optimized Cartesian coordinates for **n-tsbi3**

Center Number	Atomic Number	Atomic Type	Coordinates (Angstroms) X	Y	Z
1	6	0	3.843116	-4.037611	-0.396015
2	6	0	4.883707	-3.129664	-0.594030
3	6	0	4.667014	-1.774290	-0.394229
4	6	0	3.409906	-1.284986	-0.021147
5	6	0	2.356917	-2.206697	0.197084
6	6	0	2.596382	-3.575962	-0.001984
7	7	0	3.300933	0.108733	0.103302
8	6	0	2.237565	0.709169	-0.271202
9	6	0	1.058845	-1.791917	0.629607
10	6	0	2.096374	2.166573	-0.123110
11	6	0	0.852847	2.775699	-0.393603
12	6	0	-0.296801	1.999572	-0.750740
13	6	0	-0.057853	-1.504912	1.007172
14	6	0	3.168751	2.953704	0.303195
15	6	0	3.039039	4.330122	0.412652
16	6	0	1.820384	4.940878	0.107833
17	6	0	0.737965	4.171228	-0.292600
18	6	0	-1.284382	1.335604	-0.984076
19	6	0	-1.388213	-1.140640	1.387340
20	6	0	-2.451187	0.551875	-1.260097
21	6	0	-2.346977	-0.663672	-1.950668
22	6	0	-3.489708	-1.403975	-2.228162
23	6	0	-4.746299	-0.919634	-1.870187
24	6	0	-4.856259	0.291356	-1.189459
25	6	0	-3.713979	1.006575	-0.851597
26	6	0	-2.905747	0.384925	2.491033
27	6	0	-3.967851	-0.478511	2.228445
28	6	0	-3.745263	-1.662202	1.527143
29	6	0	-2.460729	-2.006445	1.128292
30	1	0	4.005579	-5.100604	-0.542917
31	1	0	5.862511	-3.480726	-0.905856
32	1	0	5.463928	-1.050788	-0.532688
33	1	0	1.778935	-4.269729	0.167068
34	1	0	4.109780	2.457061	0.516315
35	1	0	3.887555	4.931311	0.723500
36	1	0	1.711338	6.017512	0.195288
37	1	0	-0.220513	4.633151	-0.505888
38	1	0	1.395341	0.189170	-0.735424
39	1	0	-1.364102	-1.024983	-2.240187
40	1	0	-3.402948	-2.346394	-2.761115
41	1	0	-5.638940	-1.485803	-2.120388
42	1	0	-5.834438	0.673677	-0.911423
43	1	0	-3.786611	1.946801	-0.313413
44	1	0	-3.080361	1.317184	3.020222
45	1	0	-4.968246	-0.226718	2.568073
46	1	0	-4.570904	-2.336914	1.323368
47	1	0	-2.272369	-2.939830	0.606669
48	6	0	-1.623091	0.064512	2.064272
49	1	0	-0.788927	0.731443	2.258711

DOI:10.31579/2690-1897/217